D1.3 | Co/MgO/V/FI junctions

Author(s): Max Ilyn, Sebastian Bergeret, Celia Rogero

Delivery date: 28.02.2023
Version: 1.0

This project has received funding from the European Union's Horizon 2020 research and innovation programme under grant agreement No 800923.

Project Acronym:	SUPERTED
Project Full Title:	Thermoelectric detector based on superconductor-ferromagnet heterostructures
Call:	H2020-FETOPEN-2016-2017
Topic:	FETOPEN-01-2016-2017
Type of Action:	RIA
Grant Number:	800923
Project URL:	https://superted-project.eu/

Editor:	Maxim Ilyn, Celia Rogero, Sebastian Bergeret (CSIC). Tero Heikkilä, Sanna Rauhamäki (JYU).
Deliverable nature:	Report (R)
Dissemination level:	Public (PU)
Contractual Delivery Date:	28.02.2023
Actual Delivery Date :	28.02.2023
Number of pages:	11
Keywords:	2D magnetic materials, halides, superconductors.
Author(s):	Maxim Ilyn, CFM-CSIC Celia Rogero, CFM-CSIC
Contributor(s):	Carmen González Orellana, CFM-CSIC David Caldevilla, CFM-CSIC Elia Strambini, CNR Maria Spies, CNR Sebastian Bergeret, CFM-CSIC Stefan Ilic, CFM-CSIC
External contributor(s):	Samuel Kernsbaumer CFM-CSIC Clodoaldo I. Levartoski de Araujo, CNR Tancredi Thai Angeloni

Abstract

This deliverable 1.3 is the report of the results of last months of project regarding the growth and fabrication of the ferromagnet/superconductor (FI/S) multilayer devices. In particular, the report includes the results of the development of the 2D magnetic materials for spin-filtering tunnel barriers, as well as the use of V on V/FI bilayers

This project has received funding from the European Union's Horizon 2020 research and innovation programme under grant agreement No 800923.

1. Introduction

This report is aimed to provide the overview and present the results concerned with the Task 1.6 ”Investigate the growth of the FI thin films beyond EuS and optimize the exchange split electronic states in superconducting Al layer of the Al/FI bilayers with FI different than EuS” and the Task 1.7 ”Optimize the properties of the exchange split electronic states in superconducting V layer of the V/FI bilayers with various Fis”. Both tasks are of exploratory character and were planned to test the performance of different materials in the bilayers Superconductor (S)/ Magnetic Insulators (MI) and tunneling junctions based on these bilayers. In particular, a series of MIs were proposed to substitute EuS and superconducting material vanadium was intended as an alternative to Al. Although in the proposal we proposed the use of materials such as GdN or MgO as alternative materials for FI or tunnel barrier, the recent discovery of very interesting magnetic effects in the 2D transition metal dihalides, TMDH, took us to concentrate our exploration on this new magnetic material family. In Deliverable 1.2 [1] we introduced the reason for starting to explore these materials. In particular, these TMDH materials have the benefit of growing continuously and having a low defect density within each layer. This, along with the fact that layered magnetic compounds tend to form thin (low resistance) tunnel barriers, makes them promising candidates for use in spin-filtering barriers.

In the context of the SUPERTED project, we have considered two options for using these magnetic insulators: as a bottom layer in the tunneling junctions with Normal Ferromagnetic (NF) topmost electrode (NF/barrier/S/MI/substrate) and as a magnetic tunnel barrier in the S/MI/S junctions. In the first case, MI serves to provide the exchange coupling that creates spin split Density of States (DoS) in the superconductor. In the second case, it again creates the spin split DoS but also maintains the imbalance of the tunneling probability for the electrons with different spin orientations. Both roles are vital for the thermoelectric effect. Since optimal operation of the SUPERTED detector requires low resistance (1-10 Ω [2]) of the tunneling barriers, their thickness should be limited to 1-2 nm. This condition can be fulfilled with AlOx barriers, that we managed to make with average thickness of 2nm and resistance below 100Ω tuning the oxidation time (Fig. 1). Nevertheless, EuS films of this thickness were found to be weakly spin-filtering. Measurements performed by CNR and reported in the deliverable 2.1 [3] showed that the thickness of the EuS barrier, which provides a 50 % polarization for the 250x250 μm^2 junction gives rise to the resistance in the order of $G\Omega s$ that is far beyond the range suitable for the SUPERTED applications. Therefore, we opted for using of the magnetic 2D materials, which can provide the exchange coupling in the S/MI bilayer and serve as thin magnetic barrier in the tunneling junctions. In the deliverable 1.2 [1] we justified our decision and informed that research efforts of the tasks 1.6 and 1.7 will be centered in the implementation of the 2D magnetic materials belonging to the family of the Transition Metal DiHalides (TMDH). In the next sections, we present the report on the progress reached in this work and provide the main results.

This project has received funding from the European Union’s Horizon 2020 research and innovation programme under grant agreement No 800923.

2. Investigation of the exchange coupling between 2D magnetic semiconductor NiBr2 and superconducting Al

The first TMDH material that the CSIC group managed to fabricate in the form of thin epitaxial films was $NiBr_2$. Investigation of its electronic and magnetic properties revealed that magnetic ordering and the bandgap remain intact even in the limit of a single atomic layer [4]. In order to perform tunneling spectroscopy measurement the standard SUPERTED cross devices were fabricated but replacing the bottom EuS layer by $NiBr_2$ (Figure 1). The measurement reveals that spectra do not display the clear splitting of the superconducting DoS measured for EuS-based devices. However, the critical current of the Al wire was found to be asymmetrical with respect to the polarity of the applied current and the direction of the external magnetic field (Fig. 2 c), providing direct evidence of the exchange coupling at work.

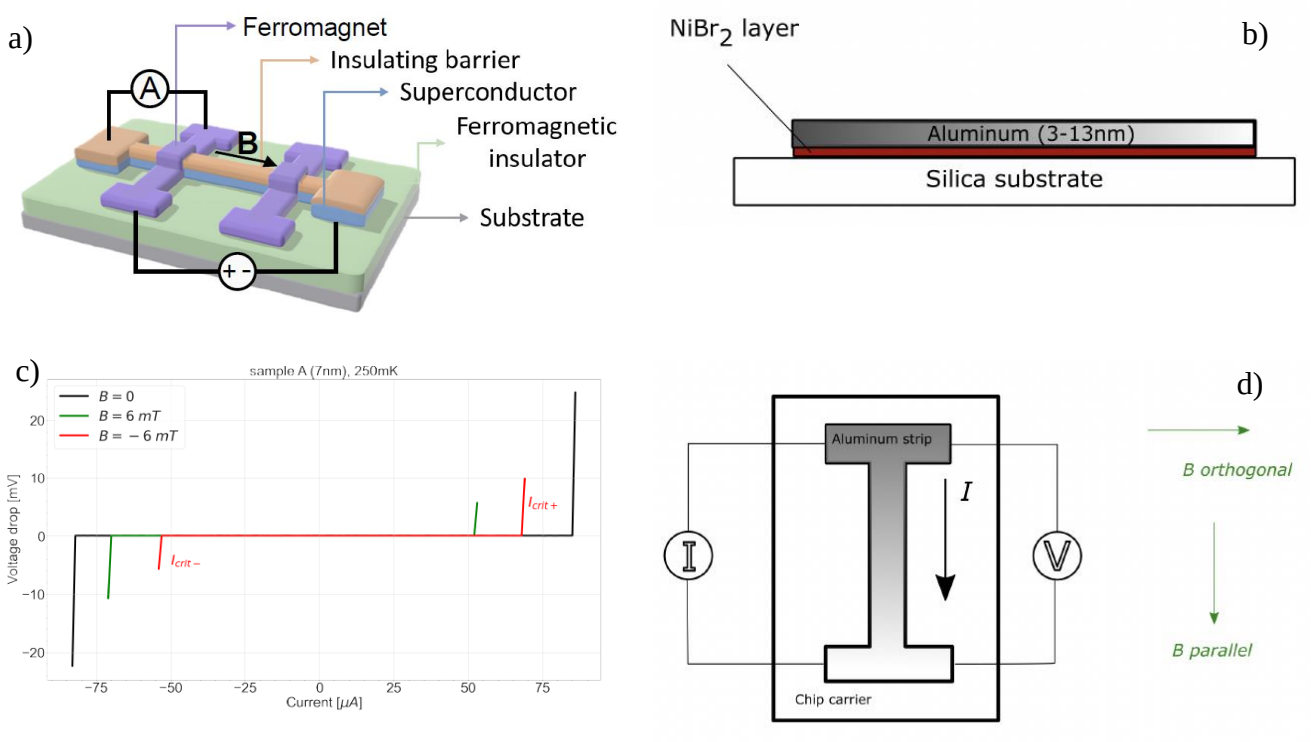

Fig. 1 (a) Schematic representation of the typical SUPERTED device comprising two tunneling junctions and having electrodes made of a ferromagnetic (top) and superconducting (bottom) metals. The superconducting electrode has spin split DoS due to the exchange coupling to the MI layer. A side view (b) and a top view (d) of the device, used to study the non-reciprocal transport properties in the Al/NiBr2 bilayer. (c) Voltage-current dependences measured via ramping of the applied voltage from zero to the positive/negative critical value resulting in the transition from superconducting to normal state.

This project has received funding from the European Union's Horizon 2020 research and innovation programme under grant agreement No 800923.

For the investigation of the exchange coupling between $NiBr_2$ and Al, CSIC group has fabricated a series of samples (Fig. 1 b and d) with variable thickness (2-12 nm) of the Al wires, as well as a test sample with additional nonmagnetic insulating layer between $NiBr_2$ and Al. Thorough study of the transport properties of these devices performed by CNR proved nonreciprocal behavior of the critical current, the effect characteristic of a superconducting diode [5,6]. Theory developed by the theoretical group of the consortium attributed this phenomenon to the non-collinear magnetic structure that appears in $NiBr_2$ below 20K [4,7].

Despite being useful for the demonstration of the exchange coupling between the 2D MI and superconductor, this magnetic texture was detrimental for creating spin-split DoS, required for the SUPERTED project. Therefore, the CSIC group proceeded with exploration of other members of the TMDH family to identify the materials with collinear magnetic order.

3. Exploration of new 2D magnetic TMDH: looking for collinear magnetic order

In order to move toward more collinear materials, we decided to explore the growth and properties of other members of the TMDH family, which, are still greatly unexplored at the few layer limit. Generating these layers at its ultimate atomic thickness will result in unprecedented fundamental properties as they retain long range magnetic order [4] and presumably exhibit a robust insulating bandgap down to the single- or double-layer thickness [8, 9]. The scarcity of information about 2D-TMDH single layers demands more fundamental research, as it hinders their implementation into devices.

Family of the TMDH magnetic transition metal dihalides consists of 18 compounds, formed by 3d transition metals (Ti, V, Mn, Fe, Co, Ni) and halides (Cl, Br, I). Table 2, extracted from ref. M. A. McGuire, Crystals 2017, 7, 121, summarizes the bulk properties of the different compounds and, those we have explored are highlighted in green.

For all of them we have tested: their chemical composition upon sublimation from submonolayer to multilayer regime; the atomic structure at the nanoscale as well as the mesoscale combining local microscopies with low-energy electron microscopies; the electronic structure at the monolayer level and the magnetic properties of the in-situ grown single and double layers; and the magnetic properties of the in-situ grown single and double slab films were measured via XAS/XMCD technique using circularly polarized synchrotron X-ray radiation. We have done this with different substrates, mainly Au(111), one of the most common substrate to study molecular and layer growth, and $NbSe_2$, one of the best known 2D superconducting surfaces. This work is still in progress and most of the data are in the analysis process or being including in publications. Therefore, in this report we are just going to highlight the relevant results, without entering in too many details.

This project has received funding from the European Union's Horizon 2020 research and innovation programme under grant agreement No 800923.

Compound	Structure Type	Reference	in Plane $M-M$ Distance (Å)	Layer Spacing (Å)	Magnetic Order	Moments in Layer	T_N, (K)	θ, (K)
$TiCl_2$	CdI_2 ($P\bar{3}m1$)	[44]	3.56	5.88	AFM	–	85	−702
$TiBr_2$	CdI_2 ($P\bar{3}m1$)	[45]	3.63	6.49	–	–	–	–
TiI_2	CdI_2 ($P\bar{3}m1$)	[46]	4.11	6.82	–	–	–	–
VCl_2	CdI_2 ($P\bar{3}m1$)	[47]	3.6	5.83	AFM	120°	36	−565, −437
VBr_2	CdI_2 ($P\bar{3}m1$)	[46]	3.77	6.18	AFM	120°	30	−335
VI_2	CdI_2 ($P\bar{3}m1$)	[48]	4.06	6.76	AFM	–	16.3, 15	−143
$MnCl_2$	$CdCl_2$ ($R\bar{3}m$)	[49]	3.71	5.86	AFM or HM	stripe or HM	2.0, 1.8	−3.3
$MnBr_2$ *	CdI_2 ($P\bar{3}m1$)	[50]	3.89	6.27	AFM	stripe $\parallel$	2.3, 2.16	–
MnI_2	CdI_2 ($P\bar{3}m1$)	[51]	4.16	6.82	HM	HM	3.95, 3.8, 3.45	–
$FeCl_2$	$CdCl_2$ ($R\bar{3}m$)	[52]	3.6	5.83	AFM	FM $\perp$	24	9 ($\parallel$), 21 ($\perp$)
$FeBr_2$	CdI_2 ($P\bar{3}m1$)	[53]	3.78	6.23	AFM	FM $\perp$	14	−3.0 ($\parallel$), 3.5 ($\perp$)
FeI_2	CdI_2 ($P\bar{3}m1$)	[54]	4.03	6.75	AFM	stripe $\perp$	9	24 ($\parallel$), 21.5 ($\perp$)
$CoCl_2$	$CdCl_2$ ($R\bar{3}m$)	[55]	3.54	5.81	AFM	FM $\parallel$	25	38
$CoBr_2$	CdI_2 ($P\bar{3}m1$)	[56]	3.69	6.12	AFM	FM $\parallel$	19	–
CoI_2	CdI_2 ($P\bar{3}m1$)	[51]	3.96	6.65	HM	HM	11	–
$NiCl_2$	$CdCl_2$ ($R\bar{3}m$)	[57]	3.48	5.8	AFM	FM $\parallel$	52	68
$NiBr_2$	$CdCl_2$ ($R\bar{3}m$)	[58]	3.7	6.09	AFM, HM	FM $\parallel$, HM	52, 23	–
NiI_2 *	$CdCl_2$ ($R\bar{3}m$)	[59]	3.9	6.54	HM	HM	75	–
$ZrCl_2$	MoS_2 ($R3m$)	[60]	3.38	6.45	–	–	–	–
ZrI_2	$MoTe_2$ ($P2_1/m$)	[61]	3.18, 3.74, 4.65	7.43	–	–	–	–
ZrI_2	WTe2 ($Pmn2_1$)	[62]	3.19, 3.74, 4.65	7.44				

Table 1 Table retrieved from Ref. 8 listing the atomic and magnetic characteristics of all TMDH family compounds. In green are highlighted the compounds we have investigated within the SUPERTED project in the monolayer limit.

By X-ray photoemission spectroscopy (XPS) we have seen that, all compounds can be deposited, in a stoichiometric form, via sublimation of the stoichiometric precursors in the UHV environment. The stoichiometry does not change with the substrate neither with the number of deposited layer, as revealed by the XPS spectra included in Fig.2 for $NiCl_2$ and $FeCl_2$ on Au(111). The advantages of this method are an ultimate control of the chemical purity and lack of flakes or contaminations typical for the exfoliated slabs. On the other hand, the technique is sufficiently simple to permit the in-situ preparation in research grade UHV chambers, but also easy to implement in manufacture processes. This method was used to deposit $NiBr_2$ on Au(111) in ref. 4.

Regarding the atomic structure, all the explored compounds exhibit a similar growth as the one previously reported for $NiBr_2$ [4]. Fig. 2 shows three Scanning tunneling microscopy (STM) images and their corresponding Low energy electron diffraction (LEED) patterns measured for three chloride compounds grown on Au(111). The images are measured for TMDH coverages ranging from 0.7 to 2 monolayers. The layer-by-layer growth is visible because the second layer (triangular features in $NiCl_2$ image) does not appear until the first layer is almost complete. Additionally, the islands grow crossing the step edges (highlighted in the image of $CoCl_2$), which indicate a low interaction with the substrate. This low interaction is also visible for the $FeCl_2$ image where the herring bond reconstruction of the Au(111) surface is perfectly distinguishable.

This project has received funding from the European Union's Horizon 2020 research and innovation programme under grant agreement No 800923.

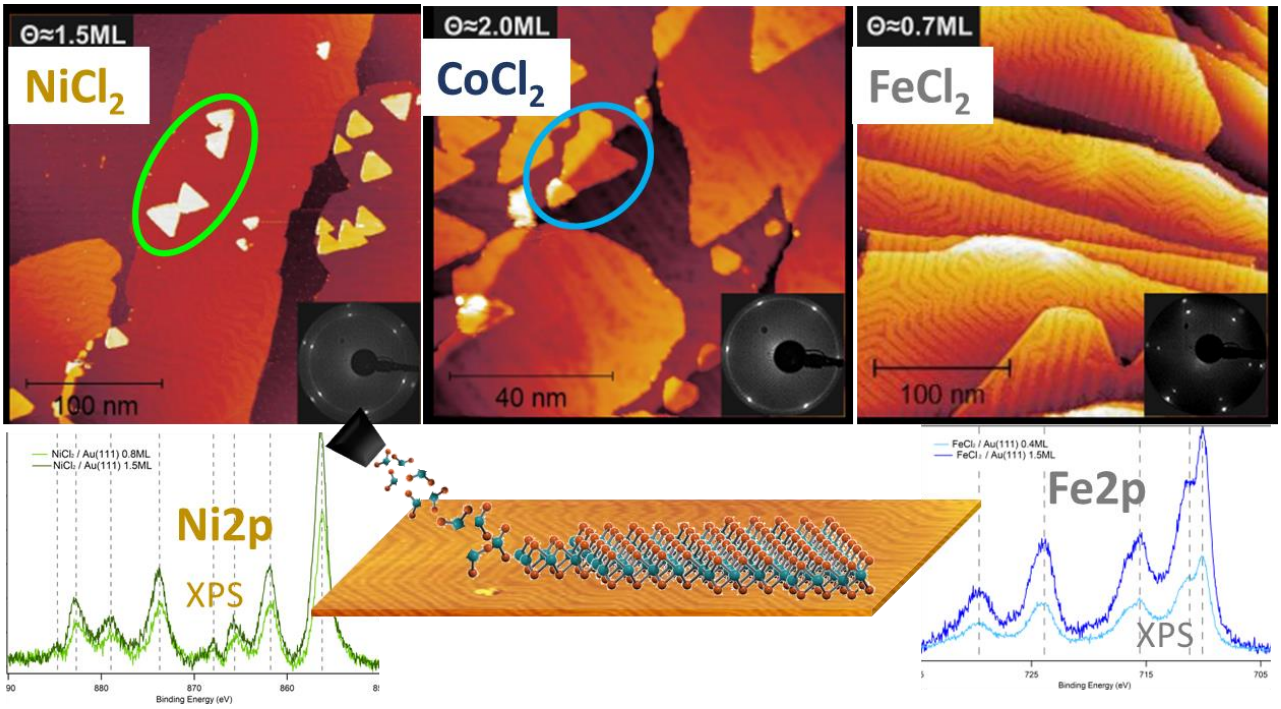

Fig. 2 Top panel: STM images of $NiCl_2$, $CoCl_2$ and $FeCl_2$ deposited on Au(111) at coverage from 0.7 to 2 monolayers. Bottom panel: Ni2p and Fe2p cover levels measured for different films of $NiCl_2$ and $FeCl_2$ grown on Au(111). In the middle the scheme for the fabrication and layer formation is also included.

XMCD measurements reveal a thickness-dependent magnetic behavior. Figure 3 shows the magnetization loops for different thicknesses and different materials extracted from the XMCD spectra. These curves were acquired sweeping the applied magnetic field ±6.5 T while measuring the x-ray absorption at the highest peak of the Fe L_3 edge. Two compounds ($NiBr_2$ and $FeBr_2$) display zero remanence characteristic of noncollinear magnetic textures. Other four compounds ($NiCl_2$, $FeCl_2$, $CoBr_2$ and $CoCl_2$) show typical ferromagnetic magnetization loops with large ($NiCl_2$, FeCl2, and $CoCl_2$) or moderate ($CoBr_2$) remanence. Field hysteresis is small and not visible in this scale. As a result of this work, we have identified four magnetic 2D compounds that possess collinear ferromagnetic order down to the single layer limit. Angle resolved photoemission spectroscopy (not shown) proved that all these compounds are insulators with a band gap of 3-4 eV. In the next section, we present the results of the first attempts to implement these compounds as a spin-filtering barrier in the tunneling junctions.

This project has received funding from the European Union's Horizon 2020 research and innovation programme under grant agreement No 800923.

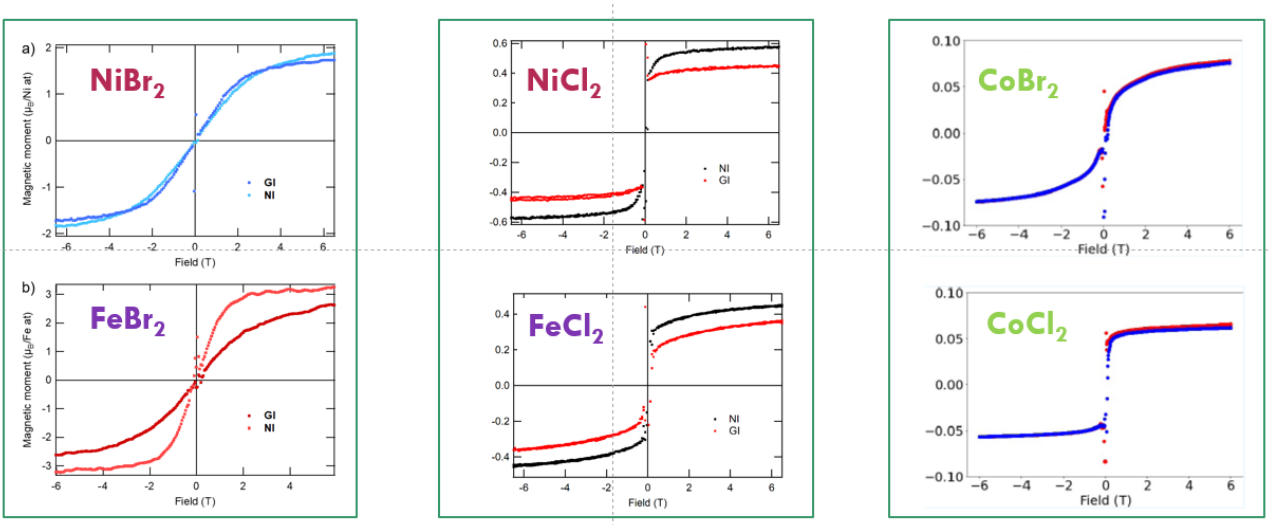

Fig.3 Magnetization loops extracted from the XMCD experiments for $NiCl_2$, $CoCl_2$ and $FeCl_2$ deposited on Au(111) at coverage from 0.7 to 2 monolayers.

4. Implementation of the V superconductor in the tunneling junctions

Before the fabrication of the TMDH-based tunneling junctions, thin films of these materials were grown on different superconducting metallic substrates and tested via XPS spectroscopy. Figure 4b shows the Xo 2p core level of $CoCl_2$ and $CoBr_2$deposited on different superconductors, Al, V and Ta, and compared to the results of the grown on Au(111). In this photoemission experiments, the changes in the spectra are associated with changes in the chemical composition. Thus, the structure of the Co2p photoemission peak characteristic of the stoichiometric $CoCl_2$/Au(111) and $CoBr_2$/Au(111) compounds changes drastically when the films are grown on Al. The position of the new peaks indicates reduction of the TMDH by Al and precipitation of metallic Co (bottom curve in the Fig. 4b). Vanadium has a minor effect on the deposited compounds while tantalum does not cause any visible reduction yielding the Co2p spectra that closely resemble the spectra of $CoCl_2$ and $CoBr_2$ obtained for the Au(111) substrate. This is a relevant result that shows that Al is not the good superconductor to interface with very thin TMDH films because it change the chemical composition of the FI and, therefore, its behaviour.

From this study we also extract that Ta is probably the best candidate to make TMDH/S devices, but, because of its extremely high sublimation temperature, the CSIC group does not have the capability of growing devices based on Ta wires. Therefore, vanadium was chosen to make devices similar to the one shown in the Fig 1a and to test the performance of the TMDH films as magnetic tunnel barriers. Table 2 summarizes parameters of the 12 fabricated devices. Three different compounds ($NiCl_2$, $CoCl_2$ and $CoBr_2$) with proven collinear ferromagnetic order were chosen for the experiment. Thickness of the barriers varied from 5 to 24 nm. First transport measurements, performed together with CNR. Even though a systematic investigation of all of the samples still

This project has received funding from the European Union's Horizon 2020 research and innovation programme under grant agreement No 800923.

needs to be done, some of the first tests have already shown some issues to overcome. For example, some of the V wires have a resistance that is higher than expected, and ohmic contact has been found between crossed V electrodes on the thinnest TMDHs barriers at temperatures down to 3 Kelvin. Observed behavior can indicate chemical reaction on the interface between the TMDH and V forming pinholes in the tunnel barrier, or degradation of the TMDH due to the exposure of the ambience because of an inadequate capping layer. Further work is necessary to identify the performance of the vanadium in the MI/S bilayers with TMDH and the Ta-based devices are foreseen to demonstrate better results.

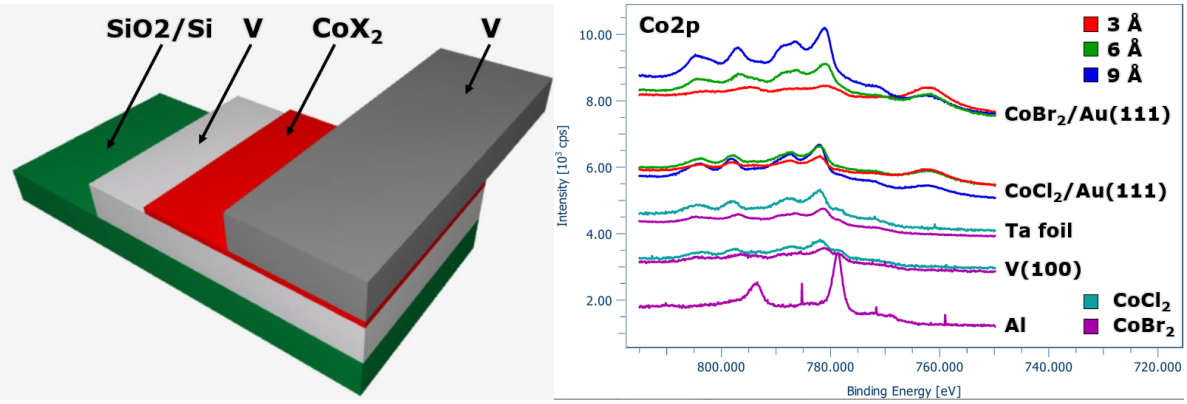

Fig. 4 (a) Schematic representation of the different layers in the V/TMDH-based tunneling junctions. (b) XPS spectroscopy of the Co2p core-level region. The spectra show results of characterization of CoCl2 and CoBr2 deposited on Al, V, Ta and Au(111) substrates.

Name	V	CoBr2	CoCl2	NiCl2
Si/SiO2/V/CoBr2/V/CaF2	12/12nm	5nm		
Si/SiO2/V/CoBr2/V/CaF2	12/12nm	7.5nm		
Si/SiO2/V/CoCl2/V/CaF2	12/12nm	5nm		
Si/SiO2/V/CoCl2/V/CaF2	12/12nm	7.5nm		
Si/SiO2/V/CoBr2/V/CaF2	10/10nm	8nm		
Si/SiO2/V/CoCl2/V/CaF2	10/10nm		8nm	
Si/SiO2/V/NiCl2/V/CaF2	10/10nm			8nm
Si/SiO2/V/CoBr2/V/CaF2	10/10nm	16nm		
Si/SiO2/V/CoBr2/V/CaF2	10/10nm	24nm		
Si/SiO2/V/CoCl2/V/CaF2	10/10nm		16nm	
Si/SiO2/V/NiCl2/V/CaF2	10/10nm			16nm
Si/SiO2/V/NiCl2/V/CaF2	10/10nm			24nm

Table 2. Parameters of the main layers in the V/TMDH/V tunnel junctions

This project has received funding from the European Union's Horizon 2020 research and innovation programme under grant agreement No 800923.

Conclusions

In this report we have presented results of the exploratory research aimed to test the performance of different materials in the superconductor/magnetic insulator (S/MI) bilayers and tunneling junctions based on these bilayers. In particular, we have investigated a series of new 2D MIs comparing the exchange coupling in the S/MI bilayers with our benchmark EuS material. We have identified that these 2D MIs can be substitutes for EuS, especially if they are used in a spin-filtering barrier configuration but the superconductor metal should be vanadium or preferably tantalum instead of aluminum because of higher chemical reactivity of the 2D MIs.

Except for solving the materials science-specific problems, developing of new materials allowed us to identify new techniques of characterization of the S/MI – based heterostructures and tunneling junctions. At the beginning of the project, tunneling spectroscopy was a default way of investigation of the exchange field, barrier polarization and other magnetic properties of our samples. The same type of characterization is widely adopted by several other groups. However, during the course of SUPERTED, studying our samples we have identified a different way of characterization of these properties based on the non-reciprocal transport measurements. On the one hand, from the non-reciprocal quasiparticle transport in tunneling junction we can extract both the exchange splitting and polarization of the quasiparticle current. On the other hand, measuring the non-reciprocal critical supercurrent we can infer whether the ferromagnetic elements have a magnetic texture, i.e. an inhomogeneous magnetization. This technique requires further development but it was found to be very useful in our research and yielded a lot of new information.

This project has received funding from the European Union's Horizon 2020 research and innovation programme under grant agreement No 800923.

Bibliography

1. Superted deliverable report 1.2.
2. Superted deliverable report 3.4.
3. Superted deliverable report 2.1.
4. D. Bikaljevic et al. “Noncollinear Magnetic Order in Two-Dimensional NiBr2 Films Grown on Au(111)”. ACS Nano 15 (2021), 14985–14995.
5. K. R. Jeon, J. K. Kim, J. Yoon, *et al.* Zero-field polarity-reversible Josephson supercurrent diodes enabled by a proximity-magnetized Pt barrier. *Nat. Mater.* **21** (2022), 1008–1013.
6. H. Narita, J. Ishizuka, R. Kawarazaki, *et al.* Field-free superconducting diode effect in noncentrosymmetric superconductor/ferromagnet multilayers. *Nat. Nanotechnol.* **17** (2022), 823–828.
7. S. Picozzi, D. Amoroso, P. Barone Spontaneous skyrmionic lattice from anisotropic symmetric exchange in a Ni-halide monolayer. Nature communication 11 (2020), 5754
8. M. A. McGuire. Crystal and magnetic structures in layered, transition metal dihalides and tri-halides. Crystals, 7(5), 2017.
9. Chhowalla, M., Shin, H., Eda, G. et al. The chemistry of two-dimensional layered transition metal dichalcogenide nanosheets. Nature Chem 5, 263–275 (2013).

This project has received funding from the European Union’s Horizon 2020 research and innovation programme under grant agreement No 800923.